Large range coherence tuned fiber optic interferometric system for application in accelerometers

A. B. L. Ribeiro,[a] J. L. Santos,[b] and D. A. Jackson
Physics Laboratory, University of Kent, Canterbury, Kent CT2 7NR, United Kingdom

(Received 18 February 1991; accepted for publication 27 February 1992)

A low coherence interferometric system with large tracking range and self-initialization to be used for remote signal processing of fiber optic accelerometers is investigated. The tracking range of the low coherence system is 1.1 mm at low frequency. Phase resolution better than 1 mrad/$\sqrt{\text{Hz}}$ at frequencies below 600 Hz is obtained, with a dynamic range of $\approx$90 dB. Data are presented which show that if the system were used to process the output from a compliant cylinder-type accelerometer, resolutions of $\sim 10^{-7}$ g/$\sqrt{\text{Hz}}$ could be achieved.

I. INTRODUCTION

The measurement of acoustic pressure, acceleration, or surface velocity is important for industrial applications and geophysical surveys. Several authors have described accelerometers[1,2] and hydrophones[3] based upon fibers wrapped around some form of compliant cylinder. In a typical arrangement the fiber forms one or both arms of the fiber optic interferometer, which may have a Mach–Zehnder or Michelson configuration. The measurand induced dimensional changes in the cylinder are transferred to the fiber inducing a phase change in the interferometer.

In order to obtain high phase resolution (10^{-6} rad/$\sqrt{\text{Hz}}$), highly coherent optical sources have been used to illuminate these systems. The sensitivity has been further enhanced by using dual compliant cylinders in a "push-pull" arrangement in the fiber Michelson configuration, as the light passes through each sensor coil twice.[1]

The "push-pull" configuration also acts to greatly reduce the sensor's cross sensitivity to temperature and pressure variations, since both cylinders are affected by these influences and the differential operation provides common mode rejection of these effects.[1] Using this approach, resolutions of better than 10^{-9} g/$\sqrt{\text{Hz}}$ have been achieved in prototype accelerometers with dynamic ranges of $\approx$100 dB. In many applications such high resolutions are not required.

As the sensitivity of the compliant cylinder accelerometer is determined by the number of fiber turns, the inertial mass, the bulk modulus, and the diameter of the cylinder, the ratio range to resolution can be tailored for a specific application. In many industrial applications for accelerometers, resolutions between 10^{-6} to 10^{-3} g/$\sqrt{\text{Hz}}$ are adequate, thus modest resolutions of only 10^{-3} to 1 rad/$\sqrt{\text{Hz}}$ are necessary for accelerometer configurations similar to those described in Refs. 1 and 2.

This level of phase resolution (10^{-3} rad/$\sqrt{\text{Hz}}$) can be readily achieved with low coherence interferometry (LCI). In the work presented here, we explore the potential performance achievable with an accelerometer simulator illuminated by a low coherence source with the induced phase changes recovered using an all-fiber receiving interferometer with a large tracking range (1.1 mm). Although resolutions obtainable using LCI are lower than obtainable using a highly coherent source, there are several advantages: (i) as the low coherence source is not affected by feedback, an isolator is not required, and (ii) the absolute value of the measurand is recoverable on "switch-on" enabling the accelerometer to be used in applications such as inertial guidance.

II. EXPERIMENT

The experimental arrangement is shown in Fig. 1. It consists of a bulk Michelson interferometer constituted by two mirrors (M) and one beamsplitter (BS), which serves as a sensor simulator, and an all-fiber (monomode) Michelson receiving interferometer, made by the directional fiber coupler (DC2). The optical source used was a multimode laser diode (ML4406), with a mean wavelength of 780 nm and a coherence length (as determined by the envelope of the visibility function) of 20 mm. The output of the laser is coupled into the monomode fiber link [using a microscope objective (Ob1) of 0.25 numerical aperture and 6 mm of operating focal length], which incorporates a nominally 50/50 directional coupler (DC1). The laser light after illuminating the sensor simulator (i.e., the bulk Michelson interferometer) is coupled back into the same fiber link by an identical microscope objective (Ob2), and transferred to the receiving interferometer via the coupler (DC1). Index-matching gel (IM) was used to eliminate the Fresnel reflection at the unused arm of the directional coupler (DC1).

The path imbalance of the bulk Michelson interferometer (i.e., the sensor simulator in Fig. 1) was set at 36.9 mm such that it exceeded the coherence length of the light source.[4] This was checked through the signal from the photodetector (D1) which showed no interference fringes. *The test signal was applied to the modulator (PZTA) in* the bulk Michelson, which had an efficiency of 0.78 rad/V.

Adjusting the path imbalances of the two interferometers to be closely matched, the signal resulting from the actuation on the PZTA can be observed (i.e., tracked by

[a]Present address: INESC, Optoelectronics Group, Largo Mompilher 22, 4000 Porto, Portugal.
[b]Permanent address: Physics Laboratory, University of Porto, Praça Gomes Teixeira, 4000 Porto, Portugal.

 0034-6748/92/073586-04$02.00

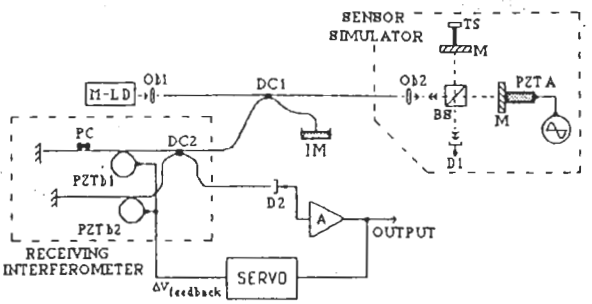

FIG. 1. Basic system with bulk Michelson sensor simulator and all-fiber receiving interferometer with tracking servo system. M-LD=multimode laser diode; PC=polarization controller; IM=index-matching gel; DC1, DC2=directional fiber couplers; Ob1, Ob2=microscope objectives; M =mirror; TS=translation stage; D1, D2=photodetectors; BS=cube beamsplitter.

the receiver) at the output of the receiving interferometer (i.e., photodetector D2). This output signal was fed into an electronic servo with a bandwidth of ≈ 1.3 kHz, which applied a voltage signal in antiphase to the two identical PZTs (PZTb1 and PZTb2), in order to maintain the system (tandem of the two interferometers) at a quadrature point on their overall transfer function.[4] The two piezoelectric cylinders in the receiving interferometer (Vernitron, PZT4 type) had an external diameter of 76 mm, wall thickness of 5 mm, and were tension wrapped with 101 turns of monomode fiber. The efficiencies of these modulators were found to be 5.61 and 6.54 rad/V for PZTb1 and PZTb2, respectively.[5] The feedback gain of the servo loop was found to be 12 rad/V (at quadrature). One polarization controller (PC) was used for the alignment of the polarization states in the two arms of the fiber Michelson interferometer in order to increase the fringe visibility of the interference signal at the output of the system (D2). The receiving interferometer was installed in a controlled environment to minimize the effects of large temperature gradients and to isolate the system from low frequency acoustic vibrations.

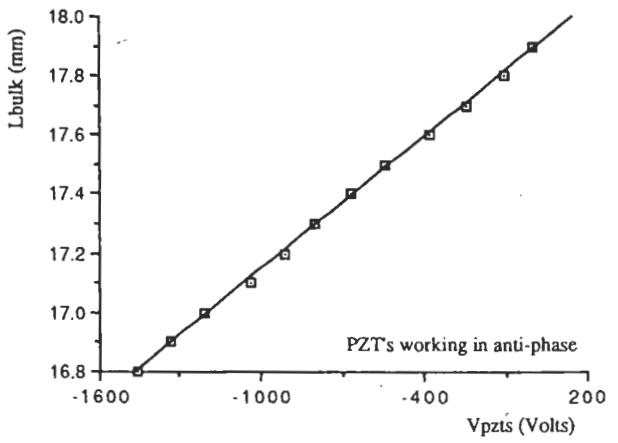

FIG. 2. Dynamic tracking range of the receiving interferometer, $\Delta L^{dyn} = 1.10$ mm $= \pm 550$ μm.

III. RESULTS AND DISCUSSION

The fringe visibility at the output of the receiving interferometer, when the system is coherently tuned to the sensor, was found to be 0.3 [the maximum possible value being 0.5 (Ref. 4)]. As one of the applications envisaged for this system is monitoring the complex vibrations of a gearbox operating at high temperature, it was necessary for the servo to have a large dynamic tracking range, in order to keep the receiving interferometer coherently tuned to the sensing interferometer. For example, for an all-fiber Michelson vibration sensor with a path imbalance of ≈ 4 cm, a temperature variation of 250 K causes the static path imbalance to change by ≈ 62 μm. The receiving system

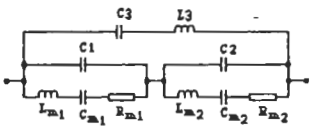

C3 = 520 pF C1 = 11.2 nF Cm1 = 1.63 nF Lm1 = 0.1634 H Rm1 = 35 Ω

L3 = 0.8 H C2 = 31.7 nF Cm2 = 2.6 nF Lm2 = 0.0752 H Rm2 = 10 Ω

(a)

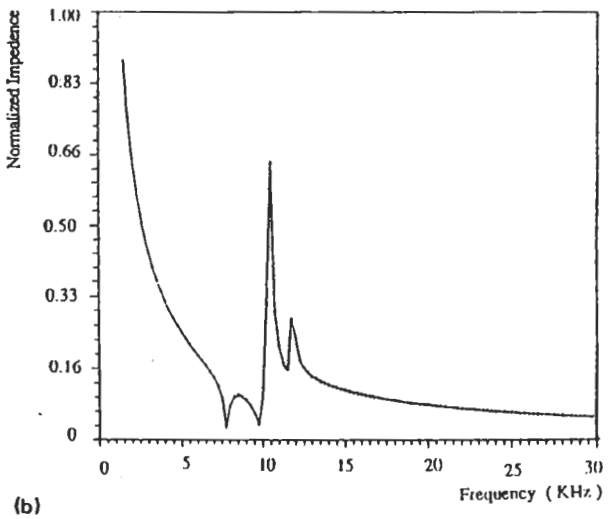

(b)

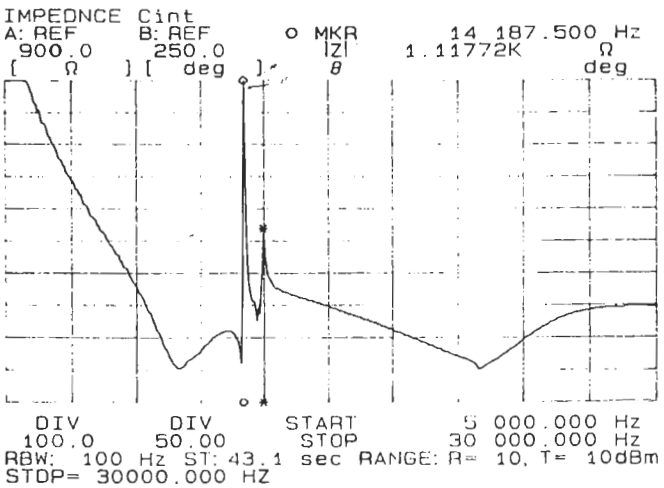

(c)

FIG. 3. (a) Theoretical model of electrical characteristics of cylindrical PZT (Vernitron PZT4). (b) Computer simulation of the variation of the PZT impedance with frequency (Vernitron PZT4). (c) Experimental measurement of the PZT impedance vs frequency.

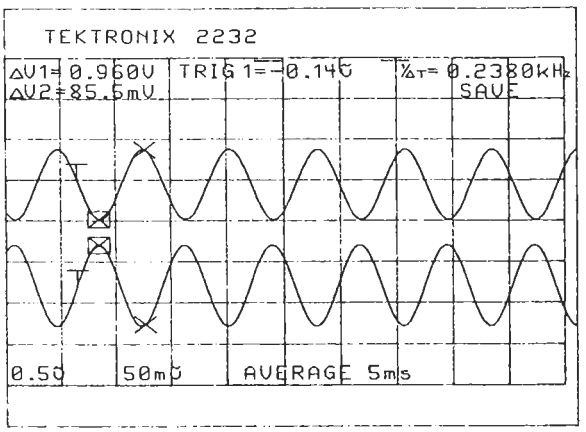

(a)

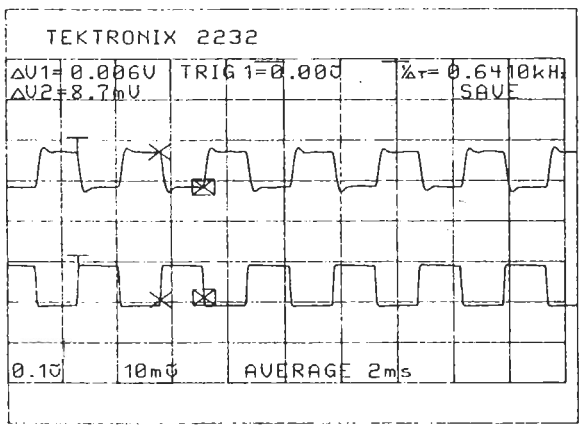

(b)

FIG. 4. System response (for ac measurements). Top traces: servo output; bottom traces: input signal. (a) 476-Hz sine wave applied to PZTA (top: 86 mV_{pp}, bottom 0.96 V_{pp}); (b) 1.28-kHz square wave applied to PZTA (top; 9.3 mV_{pp}, bottom 0.10 V_{pp}).

could track induced optical path changes in the sensor simulator up to ± 550 μm at very low frequencies, as shown in Fig. 2. However, difficulties were experienced with the system when attempting to track such large displacements at frequencies above 500 Hz. The main reason for this was the relatively low resonance frequency of the PZTs in the receiving interferometer (about 13 kHz) and the difficulty in generating very large currents required to drive the PZTs at high frequency.

To fully understand the frequency-dependent behavior of the PZTs, its electrical properties were theoretically investigated.[6] One possible equivalent circuit, with reasonable values for the circuit parameters, is shown in Fig. 3(a). The predicted performance is shown in Fig. 3(b), and Fig. 3(c) shows the experimentally determined dependence of the PZT impedance. As can be seen, the form of the two curves is similar; however, the resonance frequencies do not match exactly. This mismatch could be due to approximations in the theoretical model used. The implications of this complex behavior are currently under investigation. Clearly, the observed behavior implies that the bandwidth of the servo much be restricted to prevent it from oscillating.

The system was found to be stable with a bandwidth up to ≈ 1.3 kHz. Figures 4(a) and 4(b) show the response of the system (operating at quadrature) when PZTA in the

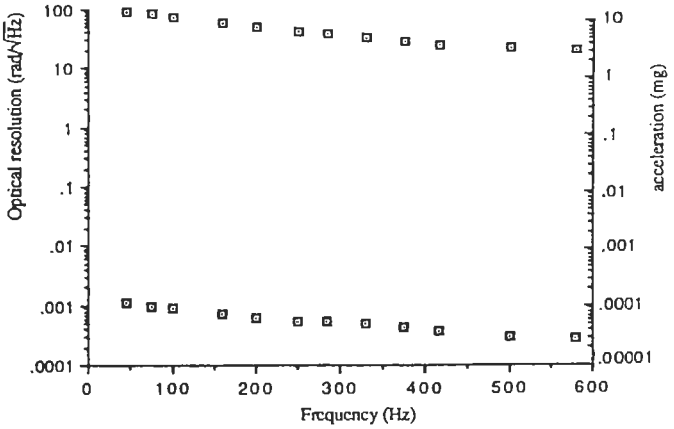

FIG. 5. System performance as a function of frequency when the system is used to interrogate a mass loaded compliant cylinder fiber optic accelerometer/geophone (Ref. 1). The lower data points give the minimum detectable phase changes and the upper data points represent the maximum tracking range of the servo. The right-hand column shows predicted resolution and maximum acceleration levels achievable when the system is used to interrogate a mass loaded compliant cylinder fiber optic accelerometer with a sensitivity of 10^4 rad/g.

bulk Michelson was driven with sinusoidal (4a) and square wave signals (4b). The resolution, for a S/N ratio of one and with the system in quadrature, was found to be better than 1 mrad/$\sqrt{\text{Hz}}$ at frequencies below 500 Hz. Also, when the amplitude of the applied signal was increased, we observed that the noise level remained the same (≈ -98 dBV). Figure 5 shows the resolution and the maximum induced phase change amplitude that the system could track. Also shown in Fig. 5 is the predicted resolution and maximum acceleration levels achievable with a compliant cylinder sensor with a sensitivity of 10^4 rad/g as reported by Gardner and Garrett.[1] A phase resolution between 1 and 0.3 mrad/$\sqrt{\text{Hz}}$ was obtained in the frequency range 30–600 Hz; the predicted acceleration resolution is better than 10^{-6} g/$\sqrt{\text{Hz}}$ throughout this range. The dynamic range of the system was ≈ 90 dB over the same frequency range, as shown in Fig. 6.

In conclusion, a coherence tuned fiber optic interferometric system with large compensating range with the ca-

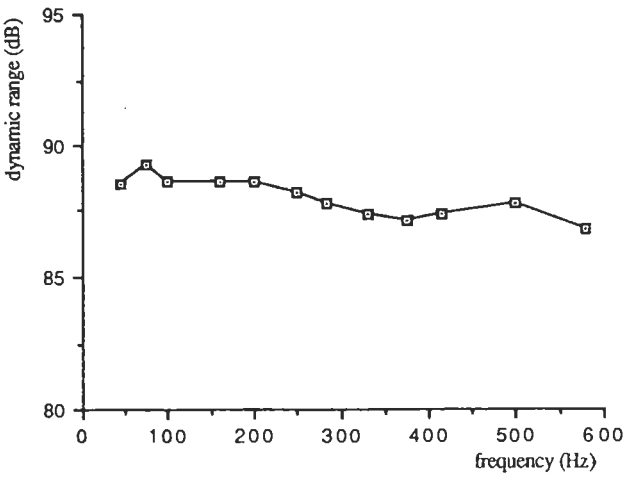

FIG. 6. Dynamic range of the system.

pacity for self-initialization has been described and experimentally investigated. Its potential application for remote signal processing of relatively modest resolution compliant cylinder-type accelerometers is addressed.

[1] D. L. Gardner and S. L. Garrett, *Fiber Optic and Laser Sensors V*, (SPIE, London, 1987), SPIE Vol. 838, p. 271.
[2] A. D. Kersey, D. A. Jackson, and M. Corke, Electron. Lett. **18**, 559 (1982).
[3] A. M. Yurek, A. B. Tveten, and A. Dandridge, in *Proceedings of the 7th OFS Conference*, Sydney, Australia (Institute of Radio and Electronics Engineers, Sydney, 1990), p. 321.
[4] D. A. Jackson and J. D. C. Jones, *Optical Fiber Sensors*, edited by J. Dakin and B. Culshaw (Artech House, Norwood, 1990), Chap. 10.
[5] G. Martini, Opt. Quantum Electron. **19**, 179 (1987).
[6] J. Zelenka, *Piezoelectric Resonators and their Applications* (Elsevier, Oxford), Vol. 24.